Earthquake Spectra, Vol.16, No.3, pp.573-592, August 2000

A Nonlinear Analysis Method for Performance Based Seismic Design

Peter Fajfar, *M.EERI*

A relatively simple nonlinear method for the seismic analysis of structures (the N2 method) is presented. It combines the pushover analysis of a multi-degree-of-freedom (MDOF) model with the response spectrum analysis of an equivalent single-degree-of-freedom (SDOF) system. The method is formulated in the acceleration - displacement format, which enables the visual interpretation of the procedure and of the relations between the basic quantities controlling the seismic response. Inelastic spectra, rather than elastic spectra with equivalent damping and period, are applied. This feature represents the major difference with respect to the capacity spectrum method. Moreover, demand quantities can be obtained without iteration. Generally, the results of the N2 method are reasonably accurate, provided that the structure oscillates predominantly in the first mode. Some additional limitations apply. In the paper, the method is described and discussed, and its basic derivations are given. The similarities and differences between the proposed method and the *FEMA 273* and *ATC 40* nonlinear static analysis procedures are discussed. Application of the method is illustrated by means of an example.

INTRODUCTION

The need for changes in the existing seismic design methodology implemented in codes has been widely recognized. The structural engineering community has developed a new generation of design and rehabilitation procedures that incorporates performance-based engineering concepts. It has been recognized (e.g., Fajfar and Krawinkler 1997) that damage control must become a more explicit design consideration. This aim can be achieved only by introducing some kind of nonlinear analysis into the seismic design methodology. In a short term, the most appropriate approach seems to be a combination of the nonlinear static (pushover) analysis and the response spectrum approach. Examples of such an approach are the capacity spectrum method, applied in *ATC 40* (ATC 1996), and the nonlinear static procedure, applied in *FEMA 273* (FEMA 1997). The later procedure is used also in *ATC 40* as an alternative method, which is called the Displacement coefficient method. Another example is the N2 method (where N stands for nonlinear analysis and 2 for two mathematical models), developed at the University of Ljubljana.

This paper deals with the N2 method. The development of the N2 method started in the mid-1980s (Fajfar and Fischinger 1987, Fajfar and Fischinger 1989). The basic idea came from the Q-model developed by Saiidi and Sozen (1981). The method has been gradually developed into a more mature version (Fajfar and Gašperšič 1996). The applicability of the method has been extended to bridges (Fajfar et al. 1997). Recently, following Bertero's (Bertero 1995) and Reinhorn's idea (Reinhorn 1997), the N2 method has been formulated in the acceleration – displacement format (Fajfar 1999). This version combines the advantages of the visual representation of the capacity spectrum method,

Faculty of Civil and Geodetic Engineering, University of Ljubljana, Jamova 2, SI-1000 Ljubljana, Slovenia

developed by Freeman (Freeman et al. 1975, Freeman 1998), with the sound physical basis of inelastic demand spectra. The inelastic spectra have been used in such a context also by Goel and Chopra (1999). The N2 method, in its new format, is in fact a variant of the capacity spectrum method based on inelastic spectra. Inelastic demand spectra are determined from a typical smooth elastic design spectrum. The reduction factors, which relate inelastic spectra to the basic elastic spectrum are consistent with the elastic spectrum. The lateral load pattern in pushover analysis is related to the assumed displacement shape. This feature leads to a transparent transformation from a multi-degree-of-freedom (MDOF) to an equivalent single-degree-of-freedom (SDOF) system.

It turns out that, if a simple alternative for the spectrum of the reduction factor is applied, the proposed method is very similar or, in a special case, even equivalent to the nonlinear static procedure presented in *FEMA 273*. The main difference with the proposed procedure compared to the procedure developed by Reinhorn (1997) is its simplicity. Reinhorn's approach is very general and less restrictive. In the proposed N2 method several simplifications have been implemented. They impose some additional limitations. On the other hand, they allow the formulation of the method in a transparent and easy-to-use format, which is convenient for practical design purposes and for the development of the future design guidelines. Although the computational procedures have been developed independently, the proposed N2 method can, in principle, be regarded as a special case of the general approach presented by Reinhorn (1997).

In the paper, the N2 method is described, its basic derivations are given, and its limitations are discussed. The similarities and differences between the proposed method and the *FEMA 273* and *ATC 40* nonlinear static analysis procedures are presented. The application of the N2 method is illustrated by means of an example.

DESCRIPTION OF THE METHOD

In this chapter, the steps of the simple version of the N2 method are described. A simple version of the spectrum for the reduction factor is applied and the influence of cumulative damage is not taken into account. It should be noted, however, that the suggested procedures used in particular steps of the method can be easily replaced by other available procedures. The complete procedure is summarized in Appendix 1.

STEP 1: DATA

A planar MDOF structural model is used. In addition to the data needed for the usual elastic analysis, the nonlinear force - deformation relationships for structural elements under monotonic loading are also required. The most common element model is the beam element with concentrated plasticity at both ends. A bilinear or trilinear moment - rotation relationship is usually used. Seismic demand is traditionally defined in the form of an elastic (pseudo)-acceleration spectrum S_{ae} (“pseudo” will be omitted in the following text), in which spectral accelerations are given as a function of the natural period of the structure T. The specified damping coefficient is taken into account in the spectrum.

STEP 2: SEISMIC DEMAND IN AD FORMAT

Starting from the acceleration spectrum, we will determine the inelastic spectra in acceleration – displacement (AD) format.

For an elastic SDOF system, the following relation applies

$$S_{de} = \frac{T^2}{4\pi^2} S_{ae} \tag{1}$$

where S_{ae} and S_{de} are the values in the elastic acceleration and displacement spectrum, respectively, corresponding to the period T and a fixed viscous damping ratio. A typical smooth elastic acceleration spectrum for 5% damping, normalized to a peak ground acceleration of 1.0 g, and the corresponding elastic displacement spectrum, are shown in Figure 1a. Both spectra can be plotted in the AD format (Figure 1b).

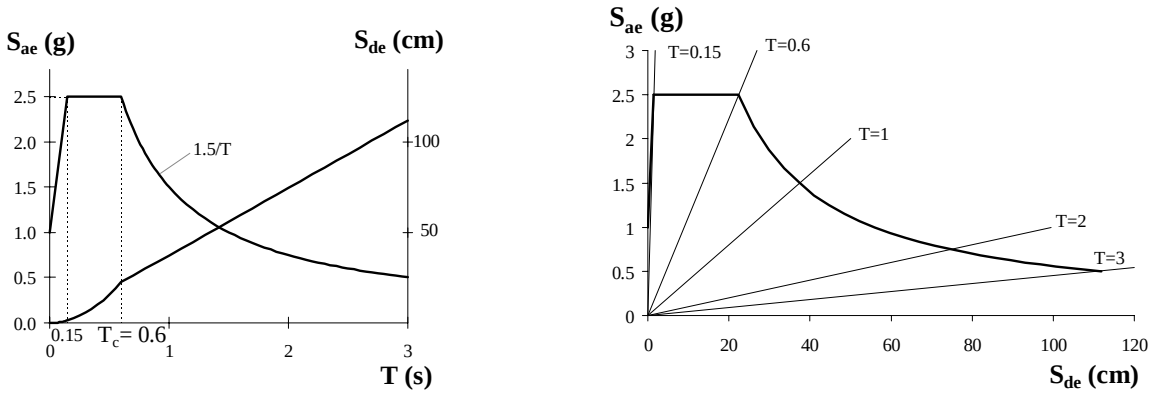

Figure 1. Typical elastic acceleration (S_{ae}) and displacement spectrum (S_{de}) for 5% damping normalized to 1.0 g peak ground acceleration. a) traditional format, b) AD format.

For an inelastic SDOF system with a bilinear force - deformation relationship, the acceleration spectrum (S_a) and the displacement spectrum (S_d) can be determined as (Vidic et al. 1994)

$$S_a = \frac{S_{ae}}{R_\mu} \tag{2}$$

$$S_d = \frac{\mu}{R_\mu} S_{de} = \frac{\mu}{R_\mu} \frac{T^2}{4\pi^2} S_{ae} = \mu \frac{T^2}{4\pi^2} S_a \tag{3}$$

where μ is the ductility factor defined as the ratio between the maximum displacement and the yield displacement, and R_μ is the reduction factor due to ductility, i.e., due to the hysteretic energy dissipation of ductile structures.

Several proposals have been made for the reduction factor R_μ. An excellent overview has been presented by Miranda and Bertero (1994). In the simple version of the N2 method, we will make use of a bilinear spectrum for the reduction factor R_μ

$$R_\mu = (\mu - 1)\frac{T}{T_C} + 1 \qquad T < T_C \tag{4}$$

$$R_\mu = \mu \qquad T \geq T_C \tag{5}$$

where T_C is the characteristic period of the ground motion. It is typically defined as the transition period where the constant acceleration segment of the response spectrum (the short-period range) passes to the constant velocity segment of the spectrum (the medium-period range). Equations 3 and 5 suggest that, in the medium- and long-period ranges, the equal displacement rule applies, i.e., the displacement of the inelastic system is equal to the displacement of the corresponding elastic system with the same period. Equations 4

and 5 represent a simple version of the formulae proposed by Vidic et al (1994). Several limitations apply. They are listed and discussed in a separate chapter entitled Limitations.

Starting from the elastic design spectrum shown in Figure 1b, and using Equations 2 to 5, the demand spectra (for the constant ductility factors μ) in AD format can be obtained (Figure 2).

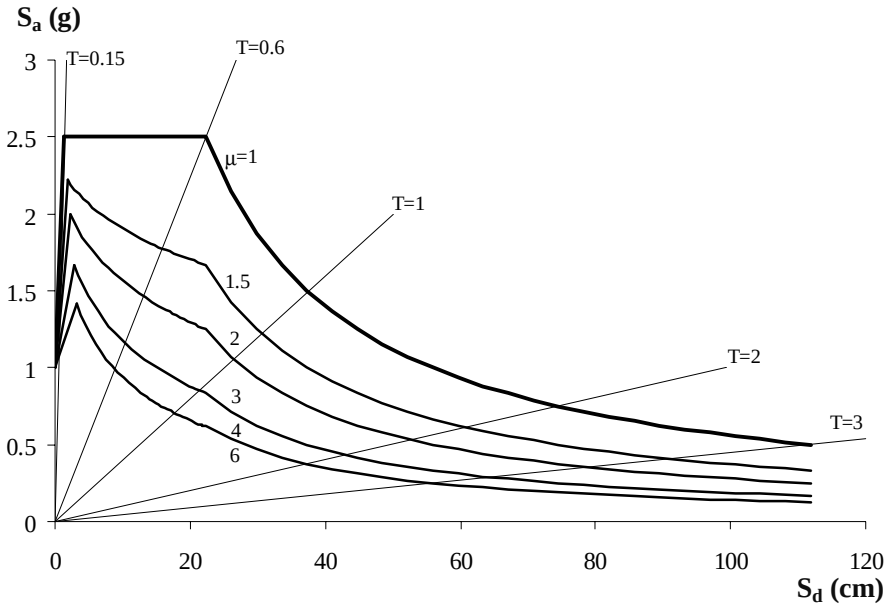

Figure 2. Demand spectra for constant ductilities in AD format normalized to 1.0 g peak ground acceleration.

The spectrum in Figure 1 has been intentionally cut off at the period T = 3 s. At longer periods the displacement spectrum is typically constant. Consequently, the acceleration spectrum in the long-period range typically decreases with the square of the period T. Depending on the earthquake and site characteristics, the constant displacement range of the spectrum may begin at even at shorter periods, e.g., at about 2 s (Tolis and Faccioli 1999). In the very-long-period range, spectral displacements decrease to the value of the peak ground displacement.

STEP 3: PUSHOVER ANALYSIS

A pushover analysis is performed by subjecting a structure to a monotonically increasing pattern of lateral forces, representing the inertial forces which would be experienced by the structure when subjected to ground shaking. Under incrementally increasing loads various structural elements yield sequentially. Consequently, at each event, the structure experiences a loss in stiffness.

Using a pushover analysis, a characteristic nonlinear force - displacement relationship of the MDOF system can be determined. In principle, any force and displacement can be chosen. In this paper, base shear and roof (top) displacement have been used as representative of force and displacement, respectively.

The selection of an appropriate lateral load distribution is an important step within the pushover analysis. A unique solution does not exist. Fortunately, the range of reasonable assumptions is usually relatively narrow and, within this range, different assumptions produce similar results. One practical possibility is to use two different displacement shapes (load patterns) and to envelope the results.

In the N2 method, the vector of the lateral loads **P** used in the pushover analysis is determined as

$$\mathbf{P} = p\,\mathbf{\Psi} = p\,\mathbf{M}\,\mathbf{\Phi} \tag{6}$$

where **M** is the diagonal mass matrix. The magnitude of the lateral loads is controlled by *p*. The distribution of lateral loads is denoted by **Ψ.** It is related to the assumed displacement shape **Φ**. Consequently, the assumed load and displacement shapes are not mutually independent as in the majority of other pushover analysis approaches. Note that Equation 6 does not present any restriction regarding the distribution of lateral loads. Usually, this distribution is assumed directly. In the proposed approach, the distribution is assumed indirectly, by assuming the displacement shape.

From Equation 6 it follows that the lateral force in the *i*-th level is proportional to the component Φ_i of the assumed displacement shape **Φ,** weighted by the story mass m_i

$$P_i = p\,m_i\,\Phi_i \tag{7}$$

Such an approach for the determination of the distribution of lateral loads has a physical background: if the assumed displacement shape was exact and constant during ground shaking, then the distribution of lateral forces would be equal to the distribution of effective earthquake forces. Moreover, by using lateral forces according to Equation 6, the transformation from the MDOF to the equivalent SDOF system and vice-versa (Steps 4 and 6) follows from simple mathematics. No additional approximations are required, as in the case in the *FEMA 273* and *ATC 40* procedures.

STEP 4: EQUIVALENT SDOF MODEL AND CAPACITY DIAGRAM

In the N2 method, seismic demand is determined by using response spectra. Inelastic behavior is taken into account explicitly. Consequently, the structure should, in principle, be modeled as a SDOF system. Different procedures have been used to determine the characteristics of an equivalent SDOF system. One of them, used in the current version of the N2 method, is discussed below.

The starting point is the equation of motion of a planar MDOF model that explicitly includes only lateral translational degrees of freedom

$$\mathbf{M}\,\ddot{\mathbf{U}} + \mathbf{R} = \mathbf{M}\,\mathbf{1}\;a \tag{8}$$

U and **R** are vectors representing displacements and internal forces, **1** is a unit vector, and *a* is the ground acceleration as a function of time. For simplicity, damping is not included in the derivation. Its influence will be included in the design spectrum.

It will be assumed that the displacement shape **Φ** is constant, i.e. that it does not change during the structural response to ground motion. This is the basic and the most critical assumption within the procedure. The displacement vector **U** is defined as

$$\mathbf{U} = \mathbf{\Phi}\,D_t \tag{9}$$

where D_t is the time-dependent top displacement. **Φ** is, for convenience, normalized in such a way that the component at the top is equal to 1.

From statics it follows

$$\mathbf{P} = \mathbf{R} \tag{10}$$

i.e., the internal forces **R** are equal to the statically applied external loads **P**.

By introducing Equations 6, 9, and 10 into Equation 8, and by multiplying from the left side with $\mathbf{\Phi}^T$, we obtain

$$\mathbf{\Phi}^T \mathbf{M} \mathbf{\Phi} \ddot{D}_t + \mathbf{\Phi}^T \mathbf{M} \mathbf{\Phi} p = -\mathbf{\Phi}^T \mathbf{M} \mathbf{1} a \tag{11}$$

After multiplying and dividing the left hand side with $\mathbf{\Phi}^T \mathbf{M} \mathbf{1}$, the equation of motion of the equivalent SDOF system can be written as

$$m^* \ddot{D}^* + F^* = -m^* a \tag{12}$$

where m^* is the equivalent mass of the SDOF system

$$m^* = \Phi^T \mathbf{M} \mathbf{1} = \sum m_i \Phi_i \tag{13}$$

and D^* and F^* are the displacement and force of the equivalent SDOF system

$$D^* = \frac{D_t}{\Gamma} \tag{14}$$

$$F^* = \frac{V}{\Gamma} \tag{15}$$

V is the base shear of the MDOF model

$$V = \sum P_i = \mathbf{\Phi}^T \mathbf{M} \mathbf{1} p = p \sum m_i \Phi_i = p m^* \tag{16}$$

The constant Γ controls the transformation from the MDOF to the SDOF model and vice-versa. It is defined as

$$\Gamma = \frac{\mathbf{\Phi}^T \mathbf{M} \mathbf{1}}{\mathbf{\Phi}^T \mathbf{M} \mathbf{\Phi}} = \frac{\sum m_i \Phi_i}{\sum m_i \Phi_i^2} = \frac{m^*}{\sum m_i \Phi_i^2} \tag{17}$$

Γ is usually called the modal participation factor. Note that the assumed displacement shape $\mathbf{\Phi}$ is normalized – the value at the top is equal to 1. Note also that any reasonable shape can be used for $\mathbf{\Phi}$. As a special case, the elastic first mode shape can be assumed. Γ is equivalent (but, in general, not equal) to PF_1 in capacity spectrum method, and to C_0 in the displacement coefficient method (*ATC 40* and *FEMA 273*).

Note that the same constant Γ applies for the transformation of both displacements and forces (Equations 14 and 15). As a consequence, the force - displacement relationship determined for the MDOF system (the V - D_t diagram) applies also to the equivalent SDOF system (the F^* - D^* diagram), provided that both force and displacement are divided by Γ. This can be visualized by changing the scale on both axes of the force – displacement diagram (see Figure 5). The initial stiffness of the equivalent SDOF system remains the same as that defined by the base shear – top displacement diagram of the MDOF system.

In order to determine a simplified (elastic - perfectly plastic) force – displacement relationship for the equivalent SDOF system, engineering judgement has to be used. In regulatory documents, some guidelines may be given.

The graphical procedure, used in the simple N2 method, requires that the post-yield stiffness is equal to zero. This is because the reduction factor R_μ is defined as the ratio of the required elastic strength to the yield strength. The influence of moderate strain hardening is incorporated in the demand spectra. It should be emphasized that moderate strain hardening does not have a significant influence on displacement demand, and that

the proposed spectra approximately apply for systems with zero or small strain-hardening (see the section with the heading Limitations).

The elastic period of the idealized bilinear system T^* can be determined as

$$T^* = 2\,\pi \sqrt{\frac{m^*\ D_y^*}{F_y^*}} \tag{18}$$

where F_y^* and D_y^* are the yield strength and displacement, respectively.

Finally, the capacity diagram in AD format is obtained by dividing the forces in the force - deformation (F^* - D^*) diagram by the equivalent mass m^*

$$S_a = \frac{F^*}{m^*} \tag{19}$$

STEP 5: SEISMIC DEMAND FOR THE EQUIVALENT SDOF SYSTEM

The seismic demand for the equivalent SDOF system can be determined by using the graphical procedure illustrated in Figure 3 (for medium- and long-period structures; for short-period structures see figure in Appendix 1). Both the demand spectra and the capacity diagram have been plotted in the same graph. The intersection of the radial line corresponding to the elastic period of the idealized bilinear system T^* with the elastic demand spectrum S_{ae} defines the acceleration demand (strength) required for elastic behavior and the corresponding elastic displacement demand. The yield acceleration S_{ay} represents both the acceleration demand and the capacity of the inelastic system. The reduction factor R_μ can be determined as the ratio between the accelerations corresponding to the elastic and inelastic systems

$$R_\mu = \frac{S_{ae}\left(T^*\right)}{S_{ay}} \tag{20}$$

Note that R_μ is not the same as the reduction (behavior, response modification) factor R used in seismic codes. The code reduction factor R takes into account both energy dissipation and the so-called overstrength. The design acceleration S_{ad} is typically smaller than the yield acceleration S_{ay}.

If the elastic period T^* is larger than or equal to T_C, the inelastic displacement demand S_d is equal to the elastic displacement demand S_{de} (see Equations 3 and 5, and Figure 3). From triangles in Figure 3 it follows that the ductility demand, defined as $\mu = S_d / D_y^*$, is equal to R_μ

$$S_d = S_{de}(T^*) \qquad T^* \geq T_C \tag{21}$$

$$\mu = R_\mu \tag{22}$$

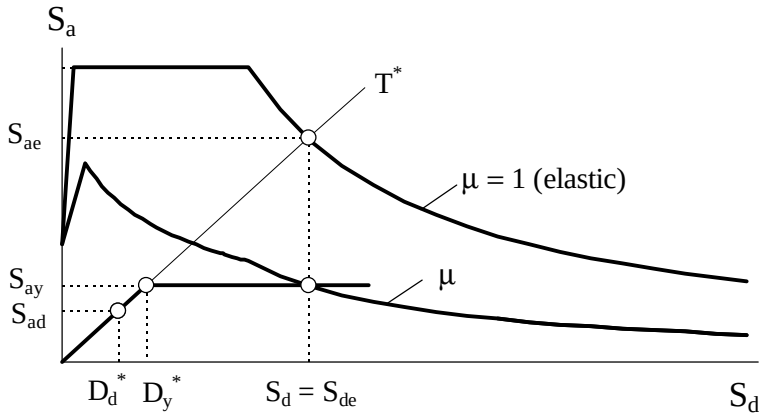

Figure 3. Elastic and inelastic demand spectra versus capacity diagram.

If the elastic period of the system is smaller than T_C, the ductility demand can be calculated from the rearranged Equation 4

$$\mu = (R_\mu - 1)\frac{T_C}{T^*} + 1 \qquad T^* < T_C \tag{23}$$

The displacement demand can be determined either from the definition of ductility or from Equations 3 and 23 as

$$S_d = \mu D_y^* = \frac{S_{de}}{R_\mu}\left(1 + (R_\mu - 1)\frac{T_C}{T^*}\right) \tag{24}$$

In both cases ($T^* < T_C$ and $T^* \geq T_C$) the inelastic demand in terms of accelerations and displacements corresponds to the intersection point of the capacity diagram with the demand spectrum corresponding to the ductility demand μ. At this point, the ductility factor determined from the capacity diagram and the ductility factor associated with the intersecting demand spectrum are equal.

Note that all steps in the procedure can be performed numerically without using the graph. However, visualization of the procedure may help in better understanding the relations between the basic quantities.

STEPS 6 AND 7: GLOBAL AND LOCAL SEISMIC DEMAND FOR THE MDOF MODEL

The displacement demand for the SDOF model S_d is transformed into the maximum top displacement D_t of the MDOF system (target displacement) by using Equation 14.

The local seismic demand (e.g., story drifts, joint rotations) can be determined by a pushover analysis. Under monotonically increasing lateral loads with a fixed pattern (as in Step 3), the structure is pushed to its target top displacement D_t determined in Step 6. It is assumed that the distribution of deformations throughout the structure in the static (pushover) analysis approximately corresponds to that which would be obtained in the dynamic analyses. Note that D_t represents a mean value for the applied earthquake loading, and that there is a considerable scatter about the mean. Consequently, it is appropriate to investigate likely building performance under extreme load conditions that exceed the design values. This can be achieved by increasing the value of the target displacement. In *FEMA 273* it is recommended to carry out the analysis to at least 150% of the calculated top displacement.

STEP 8: PERFORMANCE EVALUATION (DAMAGE ANALYSIS)

In the last step, expected performance can be assessed by comparing the seismic demands, determined in Step 7, with the capacities for the relevant performance level. The determination of seismic capacity is not discussed in this paper. Global performance can be visualized by comparing displacement capacity and demand.

LIMITATIONS

The N2 method is, like any approximate method, subject to several limitations. Applications of this method are, for the time being, restricted to the planar analysis of structures. There are two main sources of approximations and corresponding limitations: pushover analysis and inelastic spectra.

Nonlinear static (pushover) analysis can provide an insight into the structural aspects which control performance during severe earthquakes. The analysis provides data on the strength and ductility of the structure which cannot be obtained by elastic analysis. Furthermore, it exposes design weaknesses that may remain hidden in an elastic analysis. On the other hand, the limitations of the approach should be recognized. Pushover analysis is based on a very restrictive assumption, i.e. a time-independent displacement shape. Thus, it is in principle inaccurate for structures where higher mode effects are significant, and it may not detect the structural weaknesses which may be generated when the structure's dynamic characteristics change after the formation of the first local plastic mechanism. A detailed discussion of pushover analysis can be found in the paper by Krawinkler and Seneviratna (1998). Additional discussion on the relationship between MDOF and SDOF systems is presented in (Gupta and Krawinkler 2000).

One practical possibility to partly overcome the limitations imposed by pushover analysis is to assume two different displacement shapes (load patterns), and to envelope the results.

The inelastic spectra used in the proposed version of the method are based, in the medium- and long-period range, on the "*equal displacement rule*." The equal displacement rule has been used quite successfully for almost 40 years. Many statistical studies have confirmed the applicability of the rule to the medium- and long-period ranges. Only a few studies will be mentioned here.

Miranda and Bertero (1994) investigated the reduction factor R_μ proposed by eight different authors. On average, R_μ obtained for very different sets of accelerograms, recorded on firm soils, was, in the medium- and long-period ranges, roughly constant, and approximately equal to the ductility factor μ. (Note, that R_μ is equal to μ if the equal displacement rule applies.)

Vidic et al. (1994) studied the influence of hysteretic behavior, and the influence of the magnitude and model of damping on the reduction factor R_μ. On average, R_μ was roughly equal to μ in the medium- and long-period ranges. For bilinear hysteresis with 10% strain hardening, R_μ was about 20 % larger than for a stiffness-degrading hysteresis with the same post-yield slope. R_μ was also slightly larger for 2% damping than for 5% damping, and slightly larger for mass-proportional damping than for instantaneous-stiffness proportional damping.

Rahnama and Krawinkler (1993) investigated the influence of post-yield stiffness on R_μ. The results demonstrated an increase in R_μ if the post-yield stiffness increased. However, if the slope was positive (i.e., strain-hardening), the difference was relatively small. It amounted to less than 20% if the slope changed from zero to 10%.

Very recently, Miranda (2000) and Gupta and Krawinkler (2000) studied the ratio between inelastic and elastic displacement. In the Miranda's study the ideal elasto-plastic hysteretic model without strain-hardening and 5% mass-proportional damping were used. The mean value of the ratio was approximately equal to 1.0 in the medium- and long-period ranges. It has been found that for firm sites (with average shear velocities greater than 180 m/s) the influence of soil conditions can, for design purposes, be neglected. Furthermore, according to Miranda, inelastic to elastic displacement ratios were not affected by the magnitude of the earthquake event, by the level of the ground acceleration experienced at the site, or by the distance to the epicentre (near-fault ground motions are an exception). Gupta and Krawinkler studied a bilinear hysteretic system with 3% strain-hardening and 2% damping. Qualitatively, their results were very similar to those presented by Miranda. However, the mean inelastic to elastic displacement ratio according to Gupta and Krawinkler was somewhat smaller. In the medium- and long-period ranges it amounted to about 0.85.

According to Miranda (2000), the dispersion of results increases as the level of inelastic deformation increases. The values of the coefficients of variation are within the range that is typical for earthquake engineering. They are below 0.4 for $\mu = 6$ and below 0.3 for $\mu = 3$.

Based on the discussion above it can be concluded that the equal displacement rule is a viable approach for structures on firm sites with the fundamental period in the medium- or long-period range, with relatively stable and full hysteretic loops. A slightly conservative estimate of the mean value of the inelastic displacement may be obtained. The equal displacement rule, however, yields too small inelastic displacements in the case of near-fault ground motions (see, e.g., Baez and Miranda 2000), hysteretic loops with significant pinching or significant stiffness and/or strength deterioration (see e.g. Rahnama and Krawinkler 1993, and *FEMA 273*), and for systems with low strength (i.e., with a yield strength to required elastic strength ratio of less than 0.2, see Whittaker et al. 1998). Moreover, the equal displacement rule seems to be not satisfactory for soft soil conditions (see, e.g., Miranda 1993, Riddell 1995). In these cases, modified inelastic spectra should be used. Alternatively, correction factors for displacement demand (if available) may be applied.

In the case of *short-period structures*, inelastic displacements are larger than the elastic ones and, consequently, R_μ is smaller than μ. The transition period, below which the inelastic to elastic displacement ratio begins to increase, depends on the frequency content of the ground motion. For medium ductility demand ($\mu \approx 4$), it is roughly equal to the limit between the acceleration-controlled short-period range and the velocity-controlled medium-period range (i.e., to the transition period of the elastic acceleration spectrum T_C, which is also called characteristic period in this paper) (Vidic et al. 1994). It decreases and increases with a decreasing and increasing ductility factor, respectively (Vidic et al. 1994, Miranda 2000).

Equations 4 and 5 represent a simple version of the formulae for the bilinear R_μ spectrum, proposed by Vidic et al. (1994). In the original formulae, which were derived from a statistical study, the transition period (the limit between the linear and the constant segment) of the bilinear R_μ spectrum depended on ductility. In their original paper, the authors demonstrated that these formulae yield reasonably accurate displacement spectra. By assuming the transition period of the R_μ spectrum to be equal to the transition period of the elastic acceleration spectrum T_C, conservative results (i.e., higher seismic demand) are obtained for short-period structures in the case of low ductility demand ($\mu < 4$), whereas the results are slightly nonconservative for higher ductility demand. However, this assumption eliminates iteration in the short-period range, and thus greatly simplifies

the analysis procedure. (Note that the formula for the modification factor C_1 in *FEMA 273* yields the same results.)

In the short-period range, the sensitivity of inelastic displacements to changes of structural parameters is greater than in the medium- and long period ranges. Consequently, estimates of inelastic displacement are less accurate in the short-period range. However, the absolute values of displacements in the short-period region are small and, typically, they do not control the design.

POSSIBLE EXTENSIONS AND MODIFICATIONS

In this paper the simplest version of the N2 method is presented, which is subject to several limitations, discussed in the previous chapter. If needed, some extensions and modifications can be made. Research aimed at extending the applicability of the N2 method to asymmetric buildings is in progress.

In principle, any realistic elastic and corresponding (compatible) inelastic spectrum can be applied. For example, for a specific acceleration time-history, the elastic acceleration spectrum as well as the inelastic spectra, which take into account specific hysteretic behavior, can be computed and used as demand spectra. Moreover, any reasonable R_μ spectrum, compatible with the elastic spectrum, can be used. (Note that elastic spectra for specific accelerograms and smooth R_μ spectra are not compatible.) Examples are presented in (Reinhorn 1997) and (Chopra and Goel 1999).

The effect of cumulative damage can easily be taken into account by using the so-called equivalent ductility factor (e.g., McCabe and Hall 1989, Fajfar 1992). The idea behind the equivalent ductility factor is to reduce the monotonic deformation capacity of an element and/or structure as a consequence of cumulative damage due to the dissipation of hysteretic energy. Alternatively, the influence of cumulative damage can be taken into account by increasing seismic demand (e.g., Cosenza and Manfredi 1992, Chai et al. 1998).

The framework of the proposed method can, in principle, be used for the estimation of basic quantities in both force-based and displacement-based design (Fajfar 1999). Detailed procedures still have to be elaborated.

TEST EXAMPLE

As the test example the response of a four-story reinforced concrete frame building (Figure 4) subjected to three ground motion is analyzed. The full-scale building was tested pseudo-dynamically in the European Laboratory for Structural assessment (ELSA) of the Joint Research Centre of the European Commission in Ispra (Italy). The test results have been used for the validation of the mathematical model.

The building was designed according to European prestandard Eurocode 8 (CEN 1994), as a high ductility structure for a peak ground acceleration of 0.3 g. The story masses from the bottom to the top amounted to 87, 86, 86, and 83 tons, and the resulting base shear coefficient amounted to 0.15. More detailed description of the structure and mathematical modeling can be found elsewhere (e.g., Fajfar and Drobnič 1998).

Our analysis will be repeated for three levels of ground motions, with the intention of checking different performance objectives. Ground motion is defined with the elastic acceleration response spectrum according to Figure 1a, which has been normalized to a peak ground acceleration a_g equal to 0.6 g, 0.3 g (the design value), and 0.15 g, respectively.

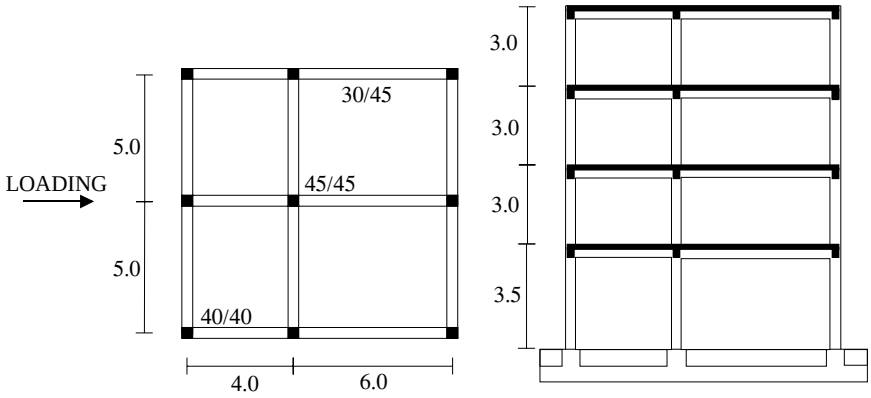

Figure 4. Test structure.

A linear displacement shape is assumed

$$\mathbf{\Phi}^T = [0.28,\ 0.52,\ 0.76,\ 1.00]$$

The lateral force pattern is obtained from Equation 6 and normalized so that the force at the top is equal to 1.0

$$\mathbf{P}^T = [0.293,\ 0.539,\ 0.787,\ 1.000]$$

With this force pattern, the DRAIN-2DX program (Prakash et al. 1993) yields the base shear V - top displacement D_t relationship shown in Figure 5.

The MDOF system is transformed to an equivalent SDOF system using Equations 14 and 15. The equivalent mass amounts to $m^* = 217$ tons (Equation 13) and the transformation constant is $\Gamma = 1.34$ (Equation 17). In Figure 5, the same curve defines both the V - D_t relationship for the MDOF system, and the force F^* - displacement D^* relation for the equivalent SDOF system. The scale of the axes, however, is different for the MDOF and SDOF systems. The factor between the two scales is equal to Γ.

A bilinear idealization of the pushover curve is shown in Figure 5. The yield strength and displacement amount to $F_y^* = 830$ kN and $D_y^* = 6.1$ cm. The elastic period is $T^* = 0.79$ s (Equation 18).

The capacity diagram (Figure 5) is obtained by dividing the forces F^* in the idealized pushover diagram by the equivalent mass (Equation 19). The acceleration at the yield point amounts to $S_{ay} = F_y^* / m^* = 830/217 = 3.82$ m/s^2 = 0.39 g.

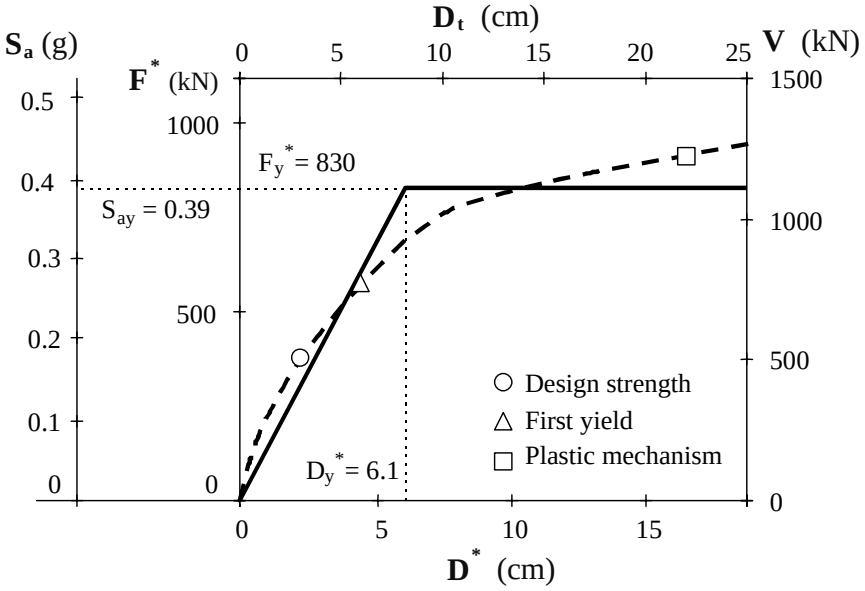

Figure 5. Pushover curve and the corresponding capacity diagram for the 4-story RC frame. Note the different scales. The top displacement D_t and the base shear V apply to MDOF system, whereas the force F^* and the displacement D^* apply to the equivalent SDOF system. The acceleration S_a belongs to the capacity diagram.

The capacity diagram and demand spectra are compared in Figure 6. Equations 1 to 5 were used to obtain the inelastic demand spectra.

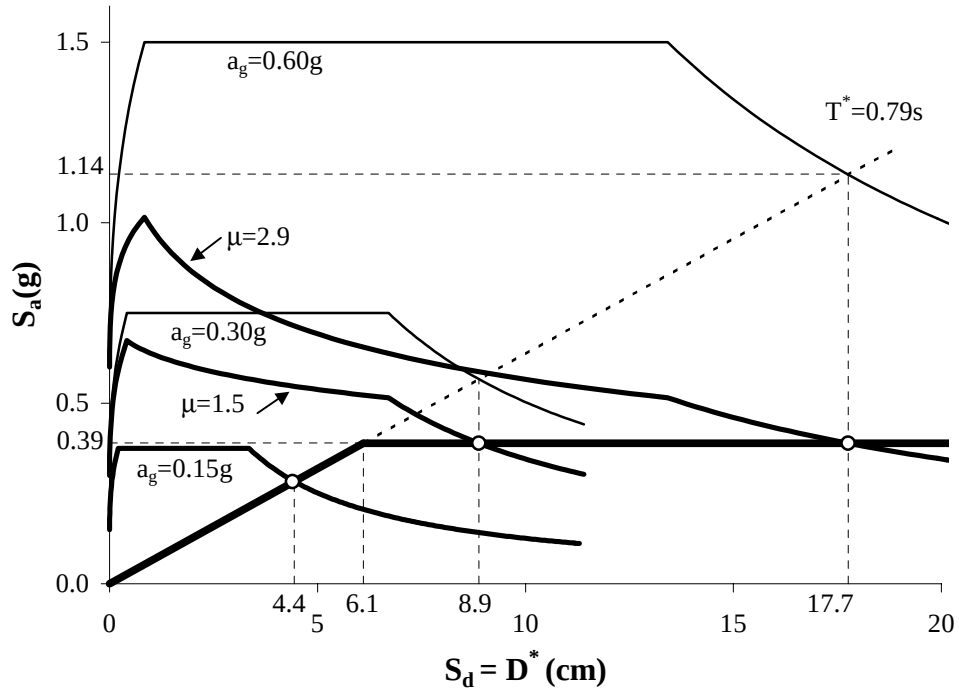

Figure 6. Demand spectra for three levels of ground motion and capacity diagram for the test example.

In the case of unlimited elastic behavior of the structure, seismic demand is represented by the intersection of the elastic demand spectrum and the line corresponding to the elastic period (T^* = 0.79 s) of the equivalent SDOF system. The values S_{ae} = 1.14 g and S_{de} = 17. 7 cm are obtained in the case of the strongest ground motion (a_g = 0.6 g). The reduction factor R_μ amounts to $R_\mu = S_{ae}/S_{ay}$ = 1.14 g/0.39 g = 2.9 (Equation 20).

The period of the system $T^* = 0.79$ is larger than T_C = 0.6. Thus the equal displacement rule (Equations 21 and 22) applies: $\mu = R_\mu = 2.9$, $S_d = S_{de} = 17.7$ cm.

The seismic demand for the equivalent SDOF system is graphically represented by the intersection of the capacity curve and the demand spectrum for $\mu = 2.9$. Note, however, that the inelastic seismic demand can be determined without constructing the inelastic demand spectra.

In the next step the displacement demand of the equivalent SDOF system is transformed back to the top displacement of the MDOF system (Equation 14): $D_t = 1.34 \cdot 17.7 = 23.7$ cm.

A pushover analysis of the MDOF model up to the top displacement D_t yields the displacement shape, local seismic demand in terms of story drifts, and joint rotations as shown in Figure 7. Envelopes of results obtained by pushing from the left to the right and in the opposite direction are shown. The results are similar to those obtained from tests and from nonlinear dynamic analyses. A comparison for a slightly different case has been presented in (Fajfar et al. 1997). In that study, the peak ground acceleration amounted to 0.45 g and damping amounted to 1% in order to allow comparison with the results of the pseudo-dynamic tests. Nonlinear dynamic analyses were performed with eight accelerograms, which roughly corresponded to the design spectrum. Considerable sensitivity to the input ground motion was observed. The results of the N2 method were within the range of results obtained by time-history analyses, and fairly close to the test results.

The next steps include assessment of seismic capacities and performance evaluation. Discussion of these steps is out of scope of this paper.

In the case of a_g = 0.3 g, the same procedure yields $S_d = S_{de} = 8.9$ cm , $\mu = 1.5$, and D_t = 11.9 cm. For a_g = 0.15 g, the following values are obtained: $S_{de} = 4.4$ cm and $D_t = 5.9$ cm. The idealized elasto-plastic structure remains in the elastic range. The original multilinear pushover curve (Figure 5) indicates that the displacement demand is approximately equal to the displacement at the first yield.

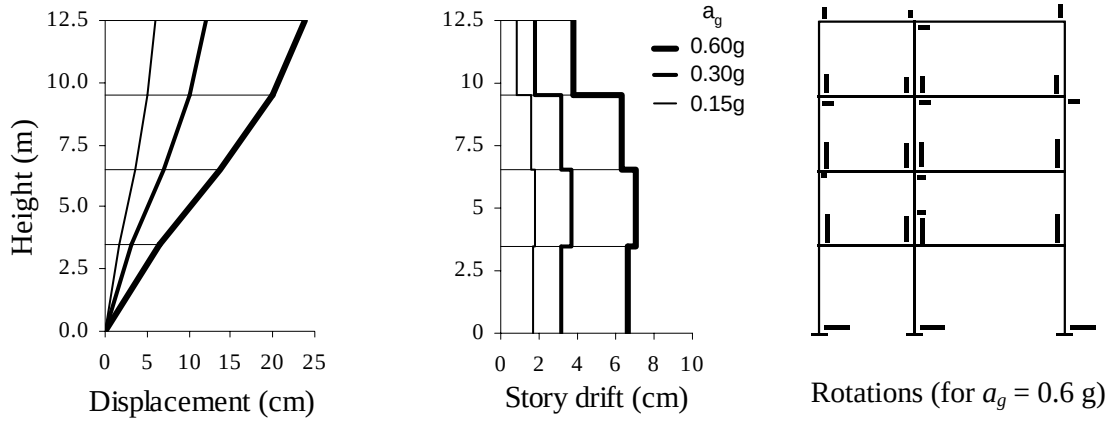

Figure 7. Displacements, story drifts, and rotations in the elements of the external frames. Rotations are proportional to the length of the mark. The maximum rotation amounts to 2.2%. Only elements which yield are indicated.

CONCLUSIONS

The N2 method can be regarded as a framework which connects pushover analysis with the response spectrum approach, and provides a tool for a rational yet practical evaluation procedure for building structures for multiple performance objectives. The

formulation of the method in the acceleration – displacement format enables the visual interpretation of the procedure and of the relations between the basic quantities controlling the seismic response. This feature may be attractive to designers. Inelastic demand spectra determined from elastic spectra by applying the reduction factor R_μ are used rather than elastic spectra with equivalent damping and period. This is the major difference with respect to the capacity spectrum method. Moreover, the transformation from a MDOF to a SDOF system is transparent, and demand quantities can be obtained without iteration. The proposed simple version of the N2 method can yield the same results as the *FEMA 273* nonlinear static procedure.

In general, the results obtained using the N2 method are reasonably accurate, provided that the structure oscillates predominantly in the first mode. Applications of the method are, for the time being, restricted to the planar analysis of structures. The inelastic demand spectra, used in the proposed simple version, are not appropriate for near-fault ground motions, for soft soil sites, for hysteretic loops with significant pinching or significant stiffness and/or strength deterioration, and for systems with low strength.

The results of the proposed method are intended to represent mean values for the applied earthquake loading. There is a considerable scatter about the mean. Consequently, it is appropriate to investigate likely building performance under extreme load conditions that exceed the design values. This can be achieved by increasing the value of the target displacement.

ACKNOWLEDGEMENTS

The results presented in this paper are based on work supported by the Ministry of Science and Technology of the Republic of Slovenia. This support is gratefully acknowledged. The author is indebted to Professor M. Fischinger for important contributions at the initial stage of development of the method, and to the past and present Ph.D. and M.Sc. students P. Gašperšič, T. Vidic, D. Drobnič, and M. Dolšek. The results of their dedicated work are included in this paper.

APPENDIX 1: SUMMARY OF THE N2 METHOD (SIMPLE VARIANT)

I. DATA

a) Structure

b) Elastic acceleration spectrum S_{ae}

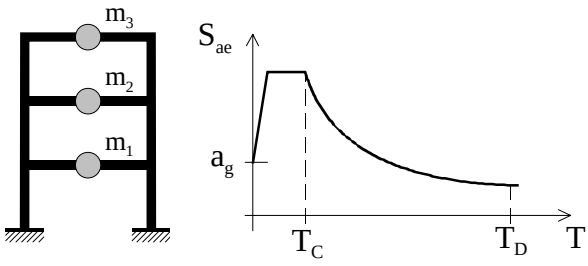

II. DEMAND SPECTRA IN AD FORMAT

a) Determine elastic spectrum in AD format

$$S_{de} = \frac{T^2}{4\pi^2} S_{ae}$$

b) Determine inelastic spectra for constant ductilities

$$S_a = \frac{S_{ae}}{R_\mu}, \quad S_d = \frac{\mu}{R_\mu} S_{de}$$

$$R_\mu = (\mu - 1)\frac{T}{T_C} + 1 \qquad T < T_C$$

$$R_\mu = \mu \qquad T \geq T_C$$

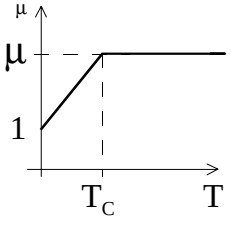

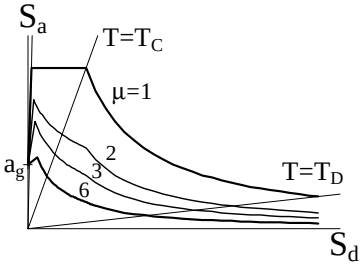

III. PUSHOVER ANALYSIS

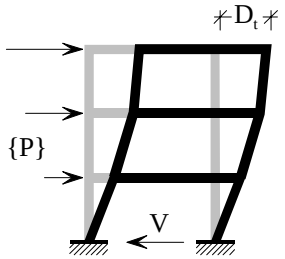

a) Assume displacement shape $\{\Phi\}$

b) Determine vertical distribution of lateral forces

$\{P\} = [M]\ \{\Phi\}, \quad P_i = m_i\ \Phi_i$

c) Determine base shear (V) – top displacement (D_t) relationship

IV. EQUIVALENT SDOF MODEL

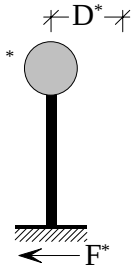

a) Determine mass m^*

$$m^* = \sum m_i\ \Phi_i$$

Note: $\Phi_n = 1.0$, n denotes roof level

b) Transform MDOF quantities (Q) to SDOF quantities (Q^*)

$$Q^* = \frac{Q}{\Gamma}, \quad \Gamma = \frac{m^*}{\sum m_i\ \Phi_i^2}$$

c) Determine an approximate elasto-plastic force – displacement relationship

d) Determine strength F_y^*, yield displacement D_y^*, and period T^*

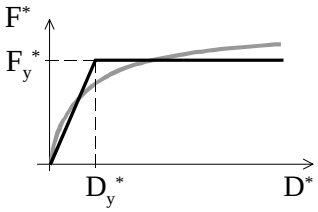

$$T^* = 2\pi\sqrt{\frac{m^*\ D_y^*}{F_y^*}}$$

e) Determine capacity diagram (acceleration versus displacement)

$$S_a = \frac{F^*}{m^*}$$

V. SEISMIC DEMAND FOR SDOF MODEL

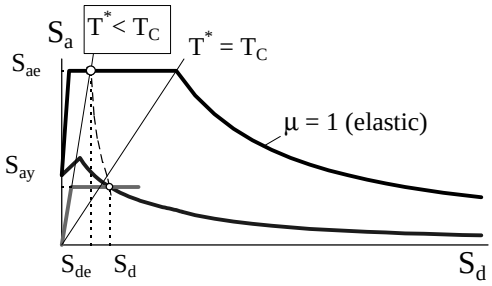

a) Determine reduction factor R_μ

$$R_\mu = \frac{S_{ae}}{S_{ay}}$$

b) Determine displacement demand $S_d = D^*$

$$S_d = \frac{S_{de}}{R_\mu}\left(1 + (R_\mu - 1)\frac{T_C}{T^*}\right) \qquad T^* < T_C$$

$$S_d = S_{de} \qquad T^* \geq T_C$$

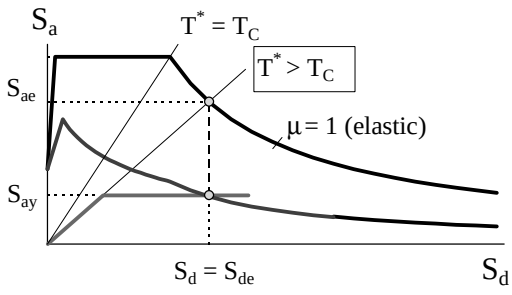

VI. GLOBAL SEISMIC DEMAND FOR MDOF MODEL

a) Transform SDOF displacement demand to the top displacement of the MDOF model

$D_t = \Gamma S_d$

VII. LOCAL SEISMIC DEMANDS

a) Perform pushover analysis of MDOF model up to the top displacement D_t (or to an amplified value of D_t)

b) Determine local quantities (e.g. story drifts, rotations Θ), corresponding to D_t

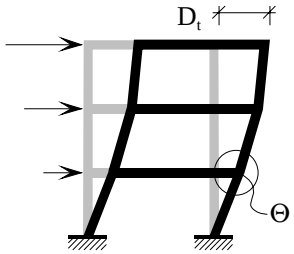

VIII. PERFORMANCE EVALUATION

a) Compare local and global seismic demands with the capacities for the relevant performance level

APPENDIX 2: COMPARISON WITH THE NONLINEAR STATIC PROCEDURE IN *FEMA 273* AND THE CAPACITY SPECTRUM METHOD IN *ATC 40*

In this chapter the basic steps of the proposed method are compared with those of the Nonlinear static procedure in *FEMA 273* and of the Capacity spectrum method in *ATC 40*. It will be shown that the proposed procedure and *FEMA 273* can yield the same results. The main difference between the proposed method and the capacity spectrum method lies in the determination of displacement demand.

PUSHOVER ANALYSIS

In *FEMA 273* and *ATC 40*, several different lateral load patterns are suggested. In the N2 method, lateral load distribution is determined by Equation 6. However, by assuming an appropriate displacement shape, any desired lateral force distribution can be obtained, including those suggested in *FEMA 273* and the basic ones in *ATC 40*.

TRANSFORMATION FROM THE MDOF TO SDOF SYSTEM

In *FEMA 273*, the transformation of displacements and forces is made using the modification factor C_o. This factor represents the "modal participation factor at the level of the control mode calculated by using a shape vector." The transformation factor Γ in the N2 method is determined by the same formula (Equation 17). Consequently, if the same displacement shape is assumed, the same transformation factor applies to both methods. In *ATC 40*, the transformation factor for displacements is the participation factor for the first mode PF_1 (if the roof level amplitude of the first mode is taken as equal to 1.0). This factor is a special case of the factors C_o and Γ, used in *FEMA 273* and the N2 method, where, in addition to the elastic first mode shape, other deformation shapes can also be used. In the capacity spectrum method, the forces in the MDOF system are directly transformed into accelerations of the SDOF system. The transformation factor is α_1. In the N2 method, this transformation is made in two steps (Equations 15 and 19). The resulting transformation factor is equal to the product $m^*\Gamma$, which is equal to α_1 if the elastic first mode shape is assumed as the displacement shape. Again, the *ATC 40* transformation is a special case of the transformation used in the N2 method.

Note, however, that in the N2 method the assumed displacement shape, used for the determination of the transformation factor Γ, also controls the distribution of lateral

forces. As a consequence, the formula for Γ (Equation 17) is derived by simple mathematics, and no additional approximations are needed. This is not the case in *FEMA 273* and *ATC 40*, where the distribution of lateral forces and displacement shape are not related.

BILINEAR IDEALIZATION OF THE PUSHOVER CURVE

Guidelines for bilinear idealization of the force-deformation relation are given in *FEMA 273*. In the N2 method, any reasonable primary slope can be used, including that determined according to *FEMA 273*. The difference in the secondary slope has no practical consequences, because it does not influence the results either in *FEMA 273* or in the N2 method, provided that it is positive (i.e., strain hardening). In *ATC 40* no idealization of the pushover curve is made.

DETERMINATION OF THE DISPLACEMENT DEMAND (TARGET DISPLACEMENT)

In *FEMA 273*, inelastic displacement demand is determined from elastic displacement demand using four modification factors. Factor C_o was discussed in the subchapter Transformation from the MDOF to SDOF system. Factor C_1 accounts for the difference in displacement demand for nonlinear response as compared with linear response for buildings with short initial vibration periods. It has the same effect as the simplified reduction factor used in the proposed version of the N2 method (Equations 4 and 5). Note that Equation 24 corresponds exactly to the equation used in *FEMA 273* in the short-period range. However, the upper limit of C_1 in *FEMA 273* is set to 1.5. In *FEMA 273*, two additional modification factors (C_2 and C_3) are used. They take into account the increase in displacement demand if hysteresis loops exhibit significant pinching (C_2) and if the post-yield slope is negative (C_3). In the case of structures with relatively stable and full hysteretic loops, C_2 =1, and if post-yield slope is positive, C_3 = 1. These effects are not considered in the proposed version of the N2 method. However, they can be easily taken into account by (a) multiplying the displacement demand by an appropriate modification factor, or by (b) dividing the reduction factors (Equations 4 and 5) by an appropriate modification factor.

The determination of seismic demand in the capacity spectrum method used in *ATC 40* is basically different. It is determined from equivalent elastic spectra. Equivalent damping and period are used in order to take into account the inelastic behavior of the structure.

CONCLUSIONS

Based on the discussions in this Appendix it can be concluded that the nonlinear static procedure in *FEMA 273* and the proposed simple version of the N2 method are very similar, and can yield exactly the same results if the same displacement shape and lateral load distribution are assumed. The major difference lies in the visualization provided by the N2 method. In *ATC 40*, the transformation from the MDOF to the SDOF system is comparable to the two other methods. However, the assumed displacement shape, which is the basic quantity in the formulae for transformation, is restricted to the elastic first mode shape. Consequently, the *ATC 40* transformation is equivalent to the *FEMA 273* and N2 transformations only in a special case. In N2, the assumed displacements shape and lateral force pattern are related. In this way one of the approximations present in *FEMA 273* and *ATC 40* is eliminated.

REFERENCES

ATC, 1996, *Seismic evaluation and retrofit of concrete buildings*, Vol. 1, ATC 40, Applied Technology Council, Redwood City, CA.

Baez, J. I. and Miranda, E., 2000, Amplification factors to estimate inelastic displacement demands for the design of structures in the near field, *Proceedings of the 12th World Conference on Earthquake Engineering*, Auckland, CD-ROM, Paper 1561, New Zealand Society for Earthquake Engineering.

Bertero, V.V., 1995, Tri-service manual methods, in *Vision 2000*, Part 2, Appendix J, Structural Engineers Association of California, Sacramento, CA.

CEN, 1994, *Eurocode 8 – Design provisions for earthquake resistance of structures*, European prestandards ENV 1998, European Committee for Standardization, Brussels.

Chai, Y. H., Fajfar, P., and Romstad, K. M, 1998, Formulation of duration-dependent inelastic seismic design spectrum, *Journal of Structural Engineering*, ASCE, **124**, 913-921.

Chopra, A. K. and Goel, R. K., 1999, Capacity-demand-diagram methods for estimating seismic deformation of inelastic structures: SDF systems, *Report PEER-1999/02*, Pacific Earthquake Engineering Research Center, University of California, Berkeley, CA.

Cosenza, E. and Manfredi, G., 1992, Seismic analysis of degrading models by means of damage functions concept, in *Nonlinear analysis and design of reinforced concrete buildings*, P. Fajfar and H. Krawinkler, Eds., Elsevier Applied Science, London and New York, 77-93.

Fajfar, P., 1992, Equivalent ductility factors, taking into account low-cycle fatigue, *Earthquake Engineering and Structural Dynamics*, **21**, 837-848.

Fajfar, P., 1999, Capacity spectrum method based on inelastic demand spectra, *Earthquake Engineering and Structural Dynamics*, **28**, 979-993.

Fajfar, P. and Drobnič, D., 1998, Nonlinear seismic analysis of the ELSA buildings, *Proceedings of the 11th European Conference on Earthquake Engineering*, Paris, CD-ROM, Balkema, Rotterdam.

Fajfar, P. and Fischinger, M., 1987, Non-linear seismic analysis of RC buildings: Implications of a case study, *European Earthquake Engineering*, **1**, 31-43.

Fajfar, P. and Fischinger, M., 1989, N2 – A method for non-linear seismic analysis of regular buildings, *Proceedings of the 9th World Conference on Earthquake Engineering*, Tokyo, Kyoto, 1988, Maruzen, Tokyo, Vol. V, 111-116.

Fajfar, P. and Gašperšič, P., 1996, The N2 method for the seismic damage analysis of RC buildings, *Earthquake Engineering and Structural Dynamics*, **25**, 23-67.

Fajfar, P., Gašperšič, P., Drobnič, D., 1997, A simplified nonlinear method for seismic damage analysis of structures, in *Seismic design methodologies for the next generation of codes*, P. Fajfar and H. Krawinkler, Eds., Balkema, Rotterdam, 183-194.

Fajfar, P. and Krawinkler, H., editors, 1997, *Seismic design methodologies for the next generation of codes*, Balkema, Rotterdam.

FEMA, 1997, *NEHRP guidelines for the seismic rehabilitation of buildings*, FEMA 273, and *NEHRP Commentary on the guidelines for the seismic rehabilitation of buildings*, FEMA 274, Federal Emergency Management Agency, Washington, D.C.

Freeman, S. A., Nicoletti, J. P., and Tyrell, J.V., 1975, Evaluations of existing buildings for seismic risk – A case study of Puget Sound Naval Shipyard, Bremerton, Washington, *Proceedings of the 1st U.S. National Conference on Earthquake Engineering*, EERI, Berkeley, CA, 113-122.

Freeman, S. A., 1998, Development and use of capacity spectrum method, *Proceedings of the 6th U.S. National Conference on Earthquake Engineering*, Seattle, CD-ROM, EERI, Oakland, CA.

Gupta, A. and Krawinkler, H., 2000, Estimation of seismic drift demands for frame structures, *Earthquake Engineering and Structural Dynamics*, **29**, in press.

Krawinkler, H. and Seneviratna, G. D. P. K., 1998, Pros and cons of a pushover analysis for seismic performance evaluation, *Engineering Structures*, **20**, 452-464.

McCabe, S. L. and Hall, W.J., 1989, Assessment of seismic structural damage, *Journal of Structural Engineering*, ASCE, **115**, 2166-2183.

Miranda, E., 1993, Site-dependent strength-reduction factors, *Journal of Structural Engineering*, ASCE, **119**, 3503-3519.

Miranda, E., 2000, Inelastic displacement ratios for displacement-based earthquake resistant design, *Proceedings of the 12th World Conference on Earthquake Engineering*, Auckland, CD-ROM, Paper 1096, New Zealand Society for Earthquake Engineering.

Miranda, E. and Bertero, V. V., 1994, Evaluation of strength reduction factors for earthquake resistant design, *Earthquake Spectra*, **10**, 357-379.

Prakash, V., Powell, G. H., and Campbell, S., 1993, DRAIN-2DX Base program description and user guide, Version 1.10, *Report No.UCB/SEMM-93/17&18*, University of California, Berkeley, CA.

Rahnama, M. and Krawinkler, H., 1993, Effects of soft soil and hysteresis model on seismic demands, *Report No. 108*, The John A. Blume Earthquake Engineering Center, Stanford University, Stanford, CA.

Reinhorn, A. M., 1997, Inelastic analysis techniques in seismic evaluations, in *Seismic design methodologies for the next generation of codes*, P. Fajfar and H. Krawinkler, Eds., Balkema, Rotterdam, 277-287.

Riddell, R., 1995, Inelastic design spectra accounting for soil conditions, *Earthquake Engineering and Structural Dynamics*, **24,** 1491-1510.

Saiidi, M. and Sozen, M. A., 1981, Simple nonlinear seismic analysis of R/C structures, *Journal of Structural Division*, ASCE, **10**7, 937-952.

Tolis, S. V. and Faccioli, E., 1999, Displacement design spectra, *Journal of Earthquake Engineering*, **3,** 107-125.

Vidic, T., Fajfar, P., and Fischinger, M., 1994, Consistent inelastic design spectra: strength and displacement, *Earthquake Engineering and Structural Dynamics*, **23**, 502-521.

Whittaker, A., Constantinou, M., and Tsopelas, P., 1998, Displacement estimates for performance-based seismic design, *Journal of Structural Engineering*, ASCE, **124**, 905-912.